

Article

Tin Removal from Tin-Bearing Iron Concentrate with a Roasting in an Atmosphere of SO₂ and CO

Lei Li ^{1,2,*}, Zhipeng Xu ² and Shiding Wang ¹

¹ Faculty of Metallurgical and Energy Engineering, Kunming University of Science and Technology, Kunming 650093, China

² College of Environmental Science and Engineering, Donghua University, Shanghai 201620, China

* Correspondence: tianxiametal1008@dhu.edu.cn; Tel.: +86-139-8761-9187; Fax: +86-21-6779-2537

Abstract: The tin could be volatilized and removed effectively from the tin-bearing iron concentrate while roasted in an atmosphere of SO₂ and CO. The reduction of SO₂ by CO occurred in preference to the SnO₂ and Fe₃O₄, and the generated S₂ could sulfurize the SnO₂ to an evaporable SnS, which resulted in the tin volatilization. However, the Fe₃O₄ could be sulfurized simultaneously, and a phase of iron sulfide was formed, retaining in the roasted iron concentrate. It decreased the quality of the iron concentrate. In addition, the formation of Sn-Fe alloy was accelerated as the roasting temperature exceeded 1100 °C, which decreased the Sn removal ratio. An appropriate SO₂ partial pressure and roasting temperature should be controlled. Under the condition of the roasting temperature of 1050 °C, SO₂ partial pressure of 0.003, CO partial pressure of 0.85, and residence time of 60 min, the tin content in the roasted iron concentrate was decreased to 0.032 wt.% and the sulfur residual content was only 0.062 wt.%, which meets the standard of iron concentrate for BF ironmaking.

Keywords: tin removal; tin-bearing iron concentrate; roasting; volatilization; SO₂ and CO



Citation: Li, L.; Xu, Z.; Wang, S. Tin Removal from Tin-Bearing Iron Concentrate with a Roasting in an Atmosphere of SO₂ and CO. *Metals* **2022**, *12*, 1974. <https://doi.org/10.3390/met12111974>

Academic Editors: Lijun Wang and Shiyuan Liu

Received: 12 October 2022

Accepted: 15 November 2022

Published: 18 November 2022

Publisher's Note: MDPI stays neutral with regard to jurisdictional claims in published maps and institutional affiliations.



Copyright: © 2022 by the authors. Licensee MDPI, Basel, Switzerland. This article is an open access article distributed under the terms and conditions of the Creative Commons Attribution (CC BY) license (<https://creativecommons.org/licenses/by/4.0/>).

1. Introduction

The Sn-bearing iron ore is a typically complex iron ore resource, with the reserve exceeding 0.5 billion tons in China [1–3]. After it is treated by traditional mineral processing technology, a Sn-bearing iron concentrate could be obtained. However, this concentrate cannot be used as a raw material for ironmaking due to the overly high tin content in it (0.3–0.8 wt %) [4]. This content exceeds the content standard of tin in the iron concentrate (<0.08 wt.%) [3,4]. To use it as a resource, much research has been carried out to remove tin from the Sn-bearing iron concentrate. Because most of the Sn phases are embedded in the iron phase at a fine-grained size, the tin could not be removed effectively through mineral processing methods [4,5]. Considering the difference between the volatility of SnO, SnS, and other phases in the Sn-bearing iron concentrate, a reduction or sulfurization roasting process has been used to remove tin from this iron concentrate [4–9]. An Fe-Sn spinel or Fe-Sn alloy was easily formed in a reduction roasting process, causing the tin removal rate to be only 80%, as reported in previous research [9,10]. By a sulfurization roasting process, the tin removal rate reached over 90% with FeS₂ [4], high-sulfur coal [6], waste tire rubber [5], or CaSO₄ [11] used as curing agents. The sulfurization roasting process might be suitable for treating the Sn-bearing iron concentrate.

In the phosphate rock processing, fuel and coal combustion, and non-ferrous and ferrous metals smelting [12–14], massive SO₂-containing gas was generated and would cause a serious pollution with an emission into the air. The treatment of SO₂ gas has received increasing attention worldwide. Processes, including the wet method [15,16], semi-dry method [17,18], dry method [19,20], and activated carbon adsorptive method [21,22], have been used to remove SO₂ from the flue gas. Among them, the CaCO₃/CaO-CaSO₄ wet method was mainly used in which the CaCO₃/CaO was firstly ground into powder, then fully mixed with water and stirred to form slurry, and at last passed into the absorption

tower together with air [16]. A high desulfurization efficiency could be obtained in this wet method; however, the generated waste gypsum residue leads a secondary pollution [15,23]. A wide variety technology is required to recycle SO_2 from flue gases, especially for the gas containing low concentration SO_2 .

The SO_2 could be reduced to elemental S_2 by CO, which could then sulfurize SnO_2 to SnS at a proper temperature [4,6,8]. Considering this, we proposed an innovative approach to remove Sn from the Sn-bearing iron concentrate using the SO_2 as the curing agent in a reducing atmosphere (CO) in this research. This research supplied a new thought for treating and reusing the low concentration SO_2 off-gas. Thermodynamic analysis and laboratory tests were carried out to study the feasibility of this approach. Furthermore, the reaction mechanism was elucidated through X-ray diffraction (XRD) and scanning electron microscopy coupled with energy dispersive spectrometry (SEM-EDS).

2. Materials and Methods

2.1. Materials

The tin-bearing iron concentrate used in this study was collected from an ironmaking plant in Yunnan province of China. The element analysis result shows that it contains 65.52 wt. % Fe and 0.39 wt.% Sn (Table 1). A pre-removal of Sn should be carried out before it used as an ironmaking raw material. Figure 1a shows that the main phase in this iron concentrate is Fe_3O_4 , and the Sn-containing phase of cassiterite (SnO_2) is embedded in this Fe_3O_4 phase as demonstrated in the electron probe microanalysis techniques (EPMA) analysis result (Figure 1b).

Table 1. Chemical composition of the Sn-bearing iron concentrate.

Element	Fe	SiO_2	Sn	Zn	CaO	Al_2O_3	Pb	Others
Content	65.52	0.91	0.39	0.04	2.30	0.87	0.1	29.87

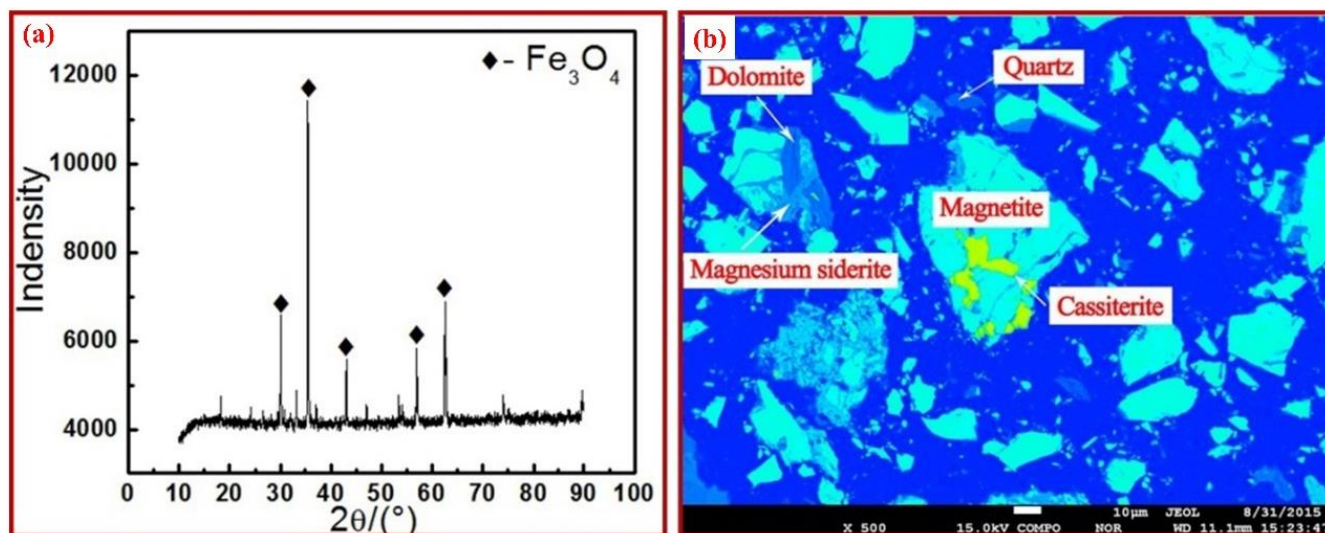


Figure 1. XRD pattern (a) and EPMA analysis (b) of the Sn-bearing iron concentrate.

The N_2 with purity of 99.99 vol.%, CO with purity of 99.99 vol.%, and mixed gas of 2 vol.% SO_2 + 98 vol.% N_2 used in this research, were supplied by the local suppliers.

2.2. Methods

The experiments were carried out in a horizontal tube furnace (GSL-1500X, Hefei Kejing Materials Technology Co. Ltd., Hefei, China), as shown in Figure 2, the temperature of which was measured by a KSY intelligent temperature controller connected to a Pt-Rh

thermocouple. For the experimental procedure, the tin-bearing iron concentrate was firstly grounded to minus 0.075 mm, placed in a crucible, transferred to the horizontal tube furnace, and heated to a proper temperature under a high-purity N₂ atmosphere with a flow rate of 40 mL/min. According to previous studies, the surface area of solid particles increased as the particle size decreased, which was beneficial to improving the gas-solid reaction area. The tin-bearing iron concentrate with particle size of 0.075 μm was selected for experiment [8]. After that, the high-purity N₂ was changed into the mixed gas of (2 vol.% SO₂ + 98 vol.% N₂) and high-purity CO at a proper volume ratio with a total flow rate of 100 mL/min, and held for a certain time. After the roasting process completed and the residue cooled down to room temperature in a high-purity N₂ atmosphere at a flow rate of 40 mL/min, the roasted residue was removed and prepared for analysis.

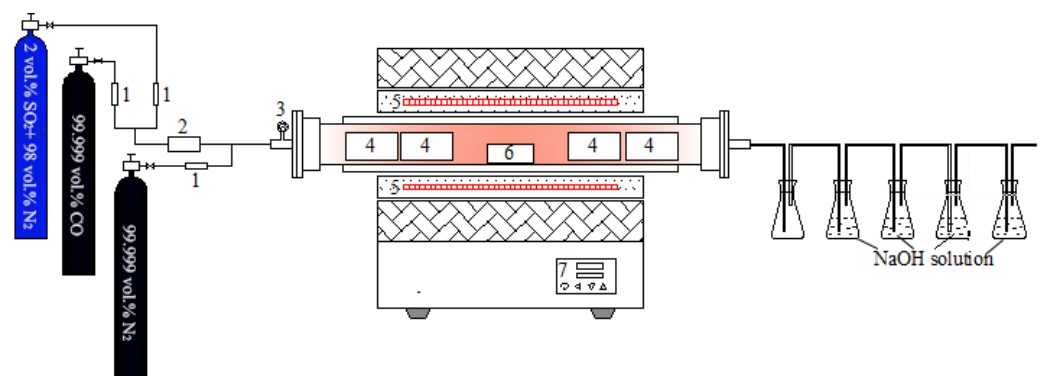


Figure 2. Schematic illustration of the experimental apparatus. (1-Mass flow meter; 2-Gas mixer; 3-Pressure gauge; 4-Filter; 5-Resistive heater; 6-Corundum reactor; 7-Temperature controller).

2.3. Characterization

Elemental composition of the samples was obtained by chemistry analytical method, all of the measurements were conducted three times and the average value was taken as the final result. The phase composition and distribution in the samples were characterized via an X-ray diffraction and EPMA techniques (JEOL, Kyoto, Japan). The XRD patterns were obtained using Cu-K α radiation in a 2 θ range of 10° to 80° with a scan step of 8°/min (Rigaku, Kyoto, Japan). In addition, FactSage 7.2 software (7.2, GTT-Technologies, Herzogenrath, Germany) was used to calculate the equilibrium phase composition during the roasting process.

Mathematical expression of the Sn volatilization ratio in this paper was defined as:

$$R = \frac{M_0 \times W_0 - M_r \times W_r}{M_0 \times W_0} \times 100\%$$

where M_0 and M_r stand for the mass of original tin-bearing iron concentrate and roasted residue, respectively, and W_0 and W_r for the Sn mass content in the original tin-bearing iron concentrate and roasted residue, respectively.

3. Thermodynamic Analysis

To investigate the effect of SO₂ (g) on the Sn volatilization rate from the tin-bearing iron concentrate under CO-SO₂ mixed atmosphere, 1 mol Fe₃O₄ and 1 mol SnO₂ were selected as the reactants to calculate the equilibrium phase composition while roasted with 2 mol CO and different amounts of SO₂ at 1100 °C using FactSage 7.2 software. Without the addition of SO₂ (g), the results in Figure 3a show that CO₂ (g), FeO, Fe₂O₃ and SnO appear, which was due to the occurrence of reactions (1)–(3). Though the decomposition of Fe₃O₄ is difficult to be carried out due to the positive value of the standard Gibbs free energy of reaction (2) at 1100 °C (Figure 3b), the occurrence of reaction (3) promoted this decomposition to happen, considering the chemical equilibrium. With the increase of the SO₂ amount from 0 to 0.4 mol, the amounts of CO (g), FeO, SnO, and Fe₂O₃ decrease, and

the amounts of CO_2 (g), S_2 (g), SnS (g), SnO_2 and Fe_3O_4 increase. In Figure 3b, the Gibbs free energy for the reduction of SO_2 (g) by CO (g) (reaction (4)) at 1100°C is minimum, causing the CO (g) amount used to reduce SnO_2 , Fe_2O_3 to be decreased in the presence of SO_2 (g) and the equilibrium amount of SnO_2 and Fe_3O_4 increased. The CO (g) first reduces SO_2 (g) to form S_2 (g) by reaction (4), and then S_2 (g) reacts with SnO (s) and SnO_2 (s) through reactions (5) and (6) to form SnS (g). The SnS (g) increases in this range of SO_2 (g) amount. With the SO_2 (g) amount exceeding 0.6 mol, an excessive SO_2 (g) exists in the equilibrium composition in Figure 3a. Consequently, the reduction of SnO_2 and Fe_2O_3 was further restrained, as a result of which the formation of SnS (g) decreased and the decomposition of Fe_3O_4 occurred little.

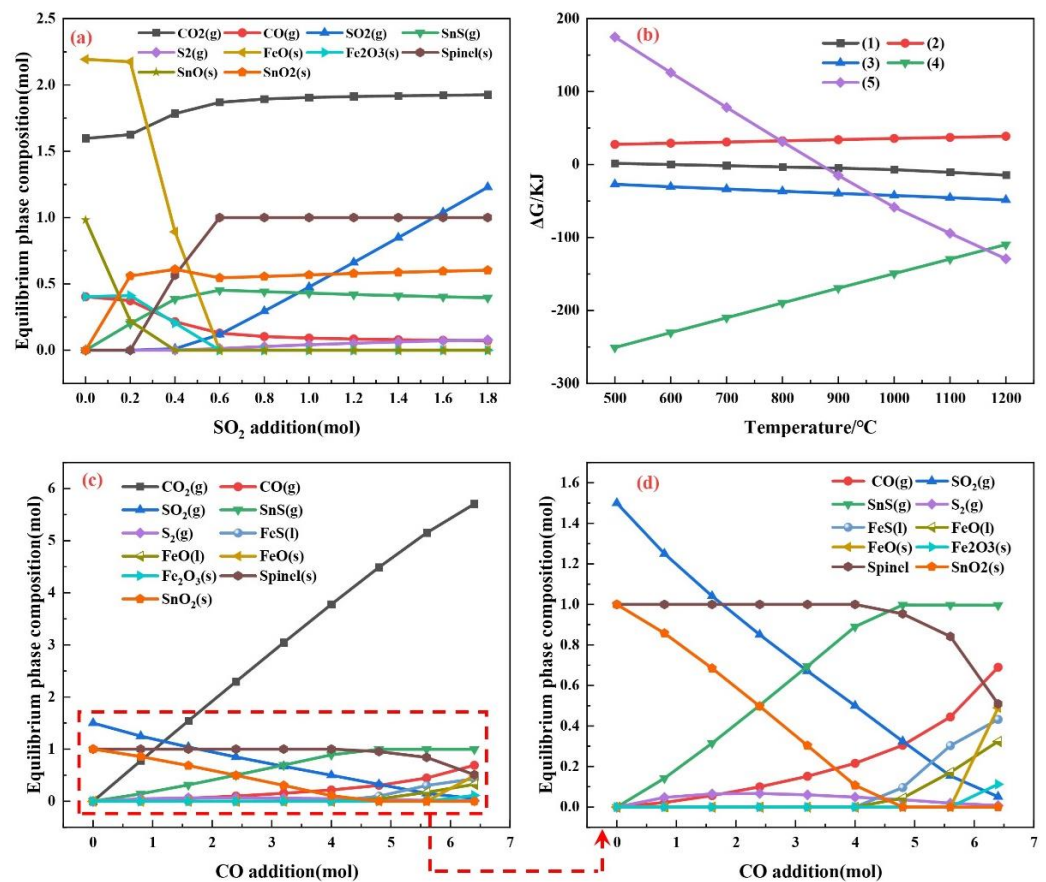
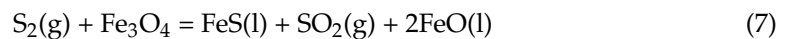
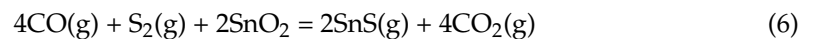
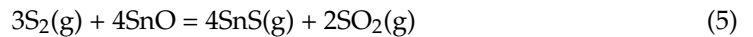
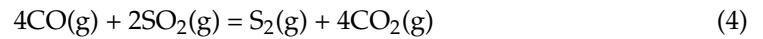
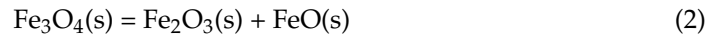
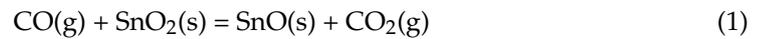


Figure 3. (a) Equilibrium phase composition of 2 mol CO + 1 mol Fe_3O_4 + 1 mol SnO_2 roasted with different amounts of SO_2 at 1100°C ; (b) Gibbs free energy changes for reaction (1)–(5) at 500 – 1100°C ; (c,d) Equilibrium phase composition of 1.5 mol SO_2 + 1 mol Fe_3O_4 + 1 mol SnO_2 roasted with different amounts of CO at 1100°C .

Under the condition of the Fe_3O_4 amount of 1 mol, SnO_2 amount of 1 mol, and SO_2 amount of 1.5 mol, the effect of CO (g) amount on the Sn transformation was then calculated at 1100°C . Figure 3c,d show that with the increase of CO amount from 0 to 5 mol, the amounts of SO_2 (g) and SnO_2 decrease accompanied with the increase of SnS (g) and S_2 (g) amounts, which might be due to the occurrence of reactions (4) to (6). As the amount of CO increases over 4 mol, the amounts of Fe_3O_4 (s) and S_2 (g) decrease while the amounts of FeO (l) and FeS (l) increase, probably due to the occurrence of reactions (4) and (7).

In summary, under the CO – SO_2 mixed atmosphere, the SnO_2 can be sulfurized and volatilized in the form of SnS (g) from the tin-bearing iron concentrate. However, some sulfur might retain in the roasted iron concentrate in form of FeS at a high CO amount,

which decreases the iron concentrate quality for ironmaking. A suitable SO_2 and CO partial pressures should be controlled during the roasting process.



4. Results and Discussion

4.1. Effects of the SO_2 Partial Pressure

Under the condition of the roasting temperature of 1000 °C, residence time of 40 min, tin-bearing iron concentrate particle size below 0.075 mm, and total flow rate of mixed gases of (2 vol.% SO_2 + 98 vol.% N_2) and high-purity CO of 100 mL/min, the effects of SO_2 partial pressure on the Sn volatilization ratio from the tin-bearing iron concentrate and S content in the roasted residue were focused firstly. The SO_2 partial pressure (P_{SO_2}) was assumed as $P_{\text{SO}_2} = V_{\text{SO}_2} / (V_{\text{SO}_2} + V_{\text{N}_2} + V_{\text{CO}})$, and the CO partial pressure (P_{CO}) was assumed as $P_{\text{CO}} = V_{\text{CO}} / (V_{\text{SO}_2} + V_{\text{N}_2} + V_{\text{CO}})$. The V_{SO_2} , V_{N_2} , and V_{CO} corresponds to the volume fraction of SO_2 , N_2 , and CO in the mixed gas respectively.

Figure 4a shows the changes of CO partial pressure (P_{CO}) with the increase of SO_2 partial pressure (P_{SO_2}) in this research. Based on it, the Fe_3O_4 and SnO_2 both could be sulfurized during the roasting process in this process, as presented the predominance area diagram of Fe-Sn-S-O at 1000 °C in Figure 4b. More S_2 (g) could be produced from the reduction of SO_2 (g) at a higher SO_2 partial pressure (P_{SO_2}) through Equation (4), which in turn could sulfurize more cassiterite (SnO_2) to SnS (g) by Equation (6). As a result, the Sn volatilization ratio increased from 60.1% to 72.4% with the P_{SO_2} from 0.001 to 0.005 as presented in Figure 4c. Furthermore, according to Figure 3c,d, the Fe_3O_4 could be sulfurized accompanied with the sulfurization of SnO_2 thermodynamically, causing the sulfur content in the roasted residue to increase with the increase of P_{SO_2} as shown in Figure 4d. Figure 5a shows the phase compositions of the roasted residues under different SO_2 partial pressures. It indicated that after the roasting treatment, the Fe_3O_4 in the raw Sn-bearing iron concentrate could be reduced into FeO at the P_{SO_2} of 0.003 and further reduced to metallic Fe as the P_{SO_2} decreased to 0.001. The CO partial pressure increased from 0.85 to 0.95 with the decrease of P_{SO_2} from 0.003 to 0.001 (Figure 4a), which promoted the further reduction of FeO to Fe. The phase of iron sulfide could not be detected in the XRD patterns of the roasted residues due to its little content. Then, an SEM-EDS analysis on the roasted residue was carried out and the result is shown in Figure 5b. In Figure 5b, the element composition of point "1" is Fe and S, which confirmed the existence of iron sulfide in the roasted residue. To increase the Sn volatilization ratio and decrease the S content in the roasted iron concentrate, the SO_2 partial pressure should be controlled at 0.003.

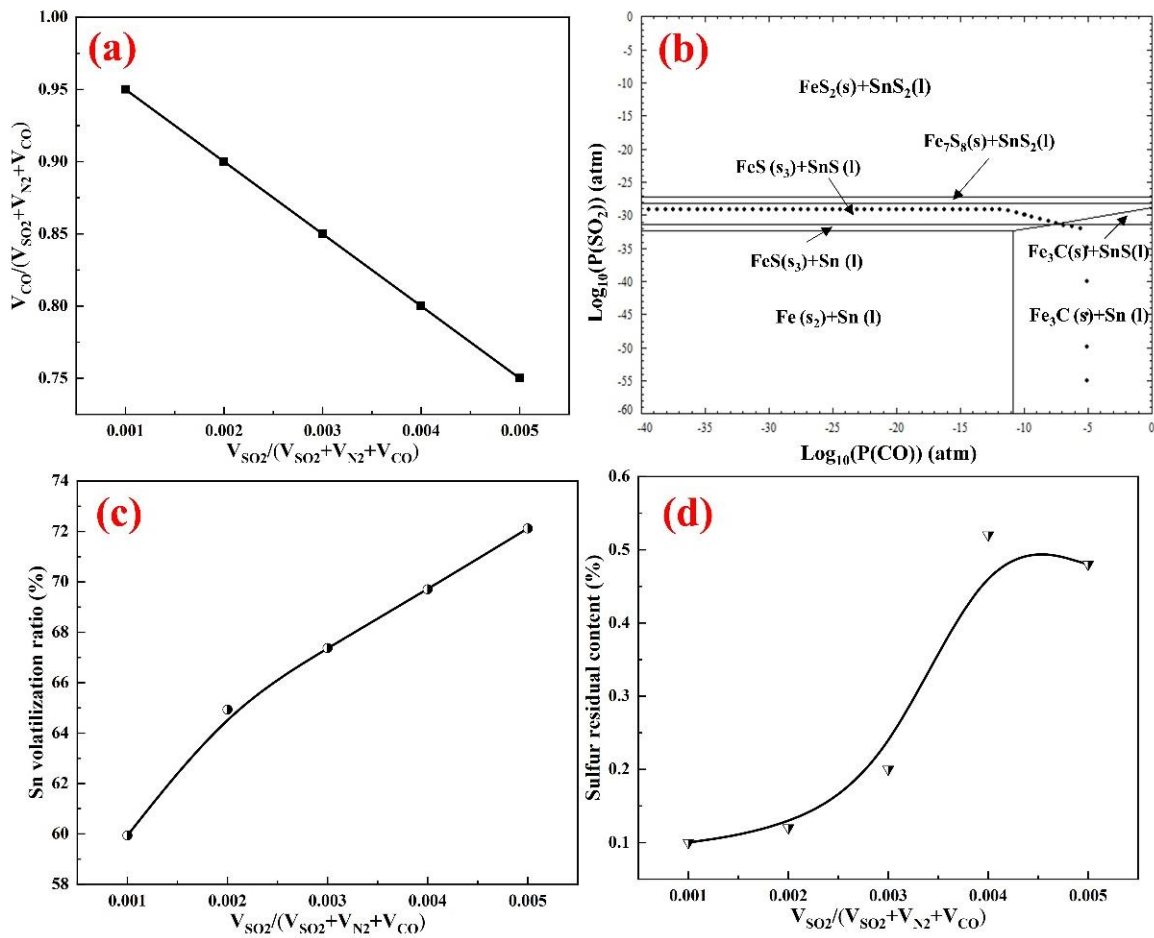


Figure 4. (a) The changes of CO partial pressure (P_{CO}) with the increase of SO_2 partial pressure (P_{SO_2}); (b) The predominance area diagram of Fe–Sn–S–O at 1000 °C; (c) Effects of SO_2 partial pressure on the Sn volatilization ratio from the tin-bearing iron concentrate; (d) The S content in the roasted iron concentrate under different SO_2 partial pressure.

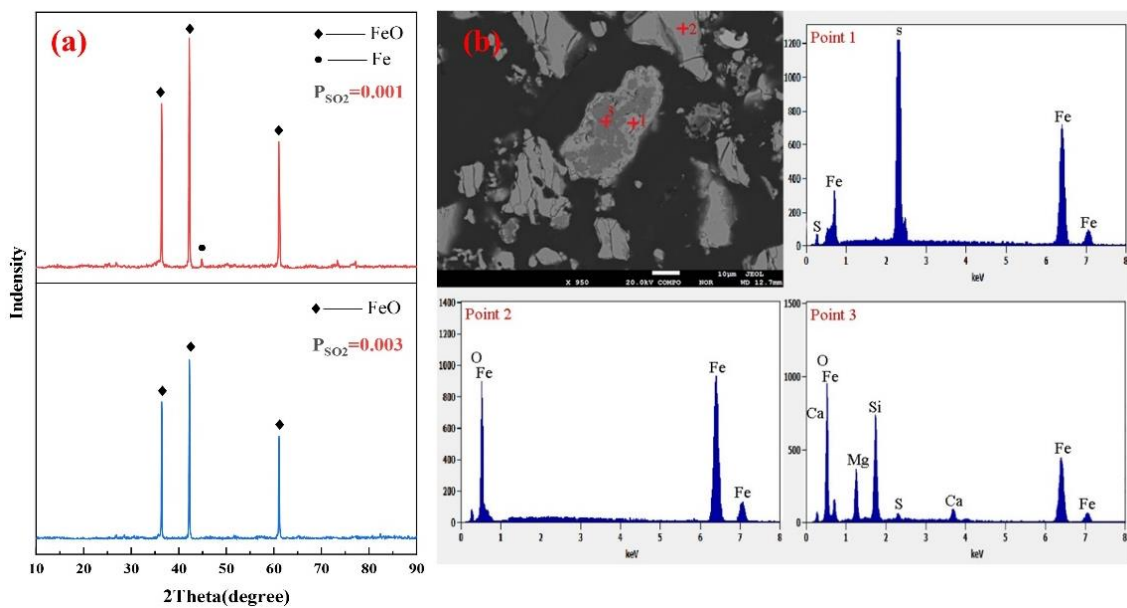


Figure 5. (a) XRD patterns of the roasted residue at the SO_2 partial pressure of 0.001 and 0.003 respectively; (b) SEM-EDS result of the roasted residue at the SO_2 partial pressure of 0.003.

4.2. Effects of Roasting Temperature

Under the condition of the SO₂ partial pressure of 0.003, residence time of 40 min, particle size of the tin-bearing iron concentrate below 0.075 mm, and total flow rate of mixed gases of (2 vol.% SO₂+ 98 vol.% N₂) and high-purity CO of 100 mL/min, the effects of roasting temperature on the Sn volatilization ratio from the tin-bearing iron concentrate and S content in the roasted residue were researched.

The sulfurization of SnO₂ through Equations (4) and (6) was accelerated at higher temperatures, and the vapor pressure of SnS (g) also increased with the increase of temperature [24]. These resulted in an increased the Sn volatilization ratio from 27.0% to 80.6% with the roasting temperature from 900 °C to 1050 °C seen in Figure 6a. However, with the roasting temperature further increased to 1100 °C, the Sn volatilization ratio decreased to 74.8%. This might be due to more generation of Fe-Sn alloy at 1100 °C, which limited the tin sulfurization and volatilization [9,10]. Comparing Figure 7a to Figure 7b, a metallic Fe phase could be detected in the roasted residue as the temperature increased from 1050 °C to 1100 °C, indicating a deeper reduction of Fe₃O₄ could be carried out and as a result more metallic Fe would be produced at a higher temperature. The generated metallic Fe might be combined with the reduced Sn to form an Fe-Sn alloy through Equation (8) [5], and more importantly the Fe content in the generated Fe-Sn alloy increased with the increase of the roasting temperature as presented in Figure 7c,d. Comparing Figure 7c to Figure 7d, the Sn content in the formed Sn-Fe alloy decreased from 97.01 wt% to 1.13 wt% as the roasting temperature increased from 900 °C to 1100 °C. The Sn activity in the Fe-Sn alloy decreased with the decrease of Sn content in it according to Raoult's law, causing the Sn sulfurization from the Fe-Sn alloy by Equation (9) to be restricted. As a result, the Sn volatilization decreased to 74.8% at 1100 °C, as shown in Figure 6a.



Similar to the sulfurization of SnO₂ through Equations (4) and (6), the transfer of 'S' from SO₂ to iron sulfide using Equation (7) was promoted with the increase of roasting temperature, causing the S content in the roasted residue increased with the temperature from 900 °C to 1000 °C (Figure 6b). However, as the temperature exceeded 1000 °C, the sulfur content in the roasted residue decreased. The reason might be that less S₂ (g) would be generated at higher temperatures deduced from Figure 3b, which in turn led to less 'S' fixed in the roasted residue in form of iron sulfide. In Figure 3b, the Gibbs free energy for reaction (4) increased with the temperature increase. Based on the results in Figure 6a,b, the optimum roasting temperature should be 1050 °C in order to maximize the removal of tin from the tin-bearing iron concentrate and to ensure a low sulfur content in the roasted residue.

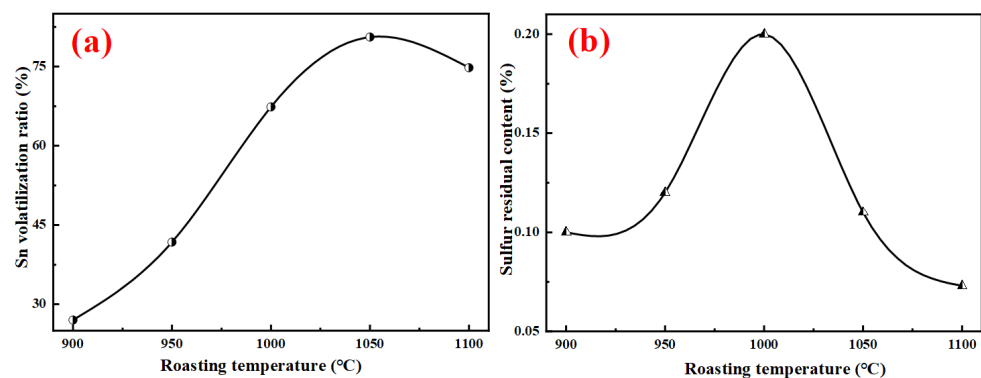


Figure 6. Effects of roasting temperature on the Sn volatilization ratio (a) from the tin-bearing iron concentrate and S content in the roasted iron concentrate (b).

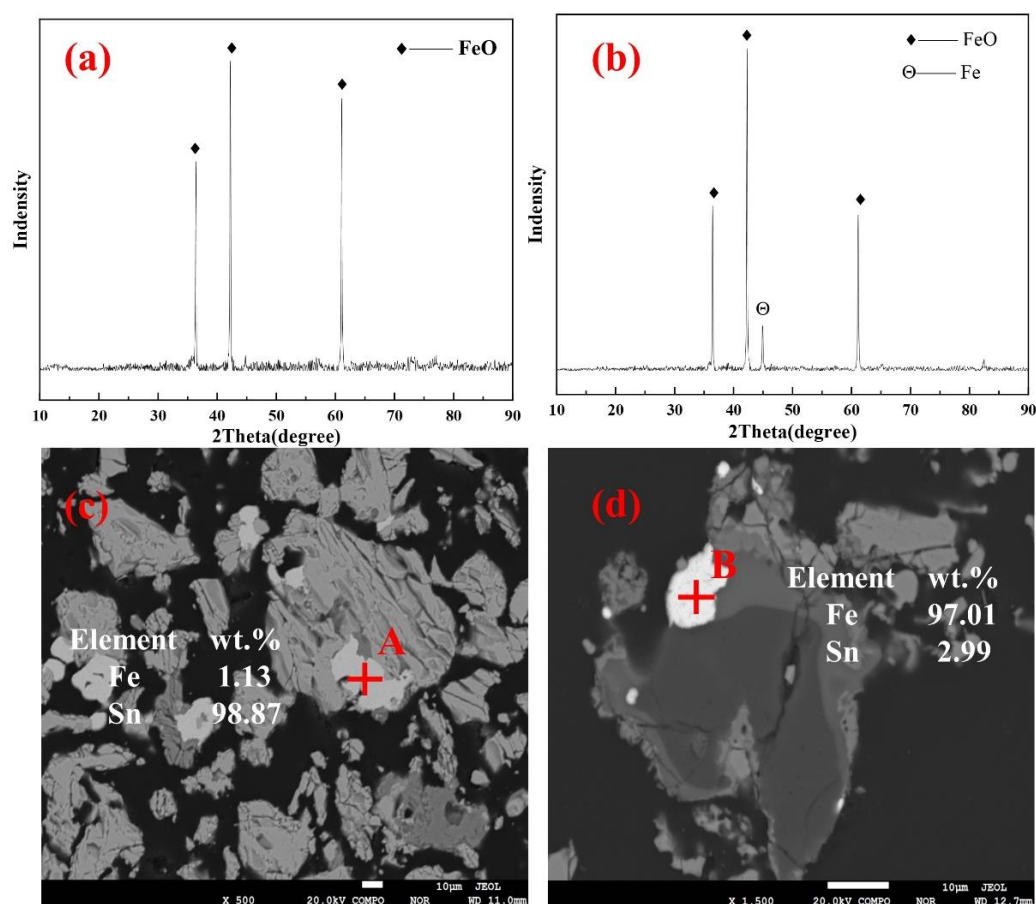


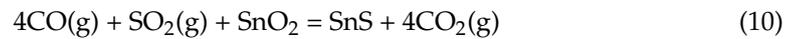
Figure 7. XRD results of the roasted residues at 1050 °C (a) and 1100 °C (b), respectively, for 40 min with the P_{SO_2} of 0.003; SEM-EDS results of the roasted residues at 1050 °C (c) and 1100 °C (d), respectively, for 40 min with the P_{SO_2} of 0.003.

4.3. Effects of the Residence Time

Under the condition of roasting temperature of 1050 °C, SO_2 partial pressure of 0.003, tin-bearing iron concentrate particle size below 0.075 mm and total flow rate of mixed gases of (2 vol.% SO_2 + 98 vol.% N_2) and high-purity CO of 100 mL/min, the effects of residence time on the Sn volatilization ratio from the tin-bearing iron concentrate and S content in the roasted residue are shown in Figure 8a,b respectively.

Based on Equations (4) and (6), the sulfurization reaction of Sn from the tin-bearing iron concentrate could be summarized as Equation (10) in this research. An unreacted core shrinking model was chosen to describe the sulfurization kinetics of SnO_2 . The reaction process could be divided into three main steps: outer diffusion of the CO and SO_2 through the gas phase boundary layer to the reactant particle surface, internal diffusion of CO and SO_2 through gaps in the reactant particle to the gas-solid reaction interface, and interfacial chemical reaction with the SnO_2 at the reaction interface. Generally, the first step of the outer diffusion is not the rate controlling step when the gas flow exceeds 60 mL/min [25,26]. The sulfurization of SnO_2 was likely controlled by the internal diffusion, interfacial chemical reaction, or the combination of them. As reported in previous research [27–29], the kinetic equations controlled by different reaction steps could be summarized in Table 2. In Table 2, the t was the reduction time, min; the X was the Sn volatilized ratio, %; and the a , b , a_1 , and b_1 were constants. With the $1 - (1 - X)^{1/3}$ used as Y-axis and t used as X-axis, the reaction would be controlled by the interfacial chemical reaction if there is a linear relationship between X and Y. Similarly, if there is a linear relationship between the $1 - 2X/3 - (1 - X)^{2/3}$ (Y-axis) and t (X-axis), the reaction would be controlled by the gas internal diffusion control; if there is a linear relationship between the $[1 + (1 - X)^{1/3} - 2(1 - X)^{2/3}]$ (Y-axis) and

$t / [1 - (1 - X)^{1/3}]$ (X -axis), the reaction would be controlled by the combination of the internal diffusion and interfacial chemical reaction.



The equations listed in Table 2 were used to treat the experimental data in Figure 8a, and the results are shown in Figure 9. In comparison with Figure 9a–c, a better linear dependence between the $1 - 2X/3 - (1 - X)^{2/3}$ (Y -axis) and t (X -axis) could be seen with the residence time from 10 min to 60 min in Figure 9a. It indicated the reaction was controlled by the gas internal diffusion control. Consequently, as the residence time increased, the CO and SO₂ gas concentration at the reaction interface gradually approached the CO and SO₂ concentration in the main gas phase, causing more of the SnO₂ to be sulfurized and volatilized. With the residence time prolonged from 20 min to 60 min, the Sn volatilization rate increased from 19.9% to 92.1%. While the residence time increased further; the Sn volatilization rate increased little. The trend in sulfur content in the roasted residue is similar with that of Sn volatilization ratio as presented in Figure 8a, which raised rapidly from 20 min to 60 min and then increased slowly as the residence time continued to increase. Considering the results in Figure 8a,b, the residence time was chosen at 60 min.

Under the condition of the roasting temperature of 1050 °C, SO₂ partial pressure of 0.003, CO partial pressure of 0.85, and residence time of 60 min, the tin removal rate from the tin-bearing iron concentrate achieved 92.1% and the Sn content in the roasted iron concentrate was decreased to 0.032 wt.%. In addition, the sulfur content in the iron concentrate is only 0.062 wt.%, which meets the standard of BF ironmaking.

Table 2. Kinetic equations for different controlling steps.

Controlling Step	Kinetic Equation [26]
Interfacial chemical reaction	$t = a [1 - (1 - X)^{1/3}]$
Gas internal diffusion	$t = b [1 - 2X/3 - (1 - X)^{2/3}]$
Combination of interfacial chemical reaction and gas internal diffusion	$t = a_1 [1 - (1 - X)^{1/3}] + b_1 [1 - 2X/3 - (1 - X)^{2/3}]$

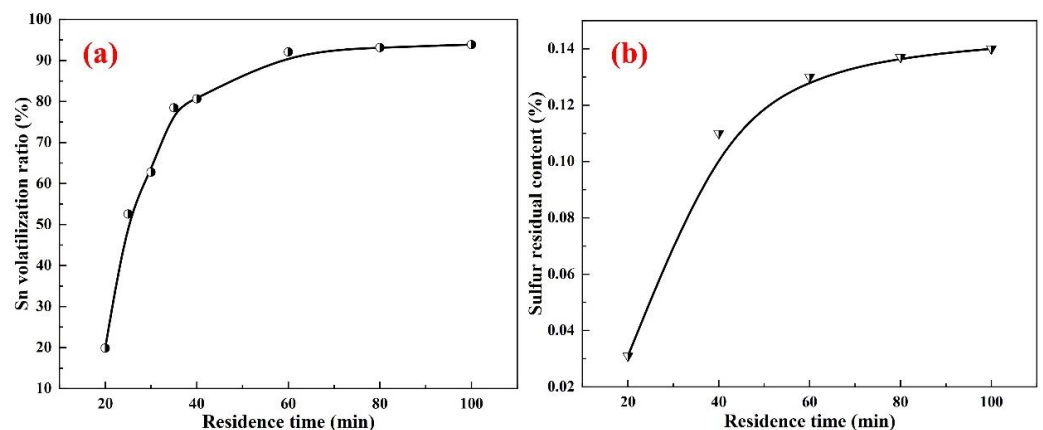


Figure 8. Effect of residence time on Sn volatilization ratio from the tin-bearing iron concentrate (a) and S content in the roasted residue (b).

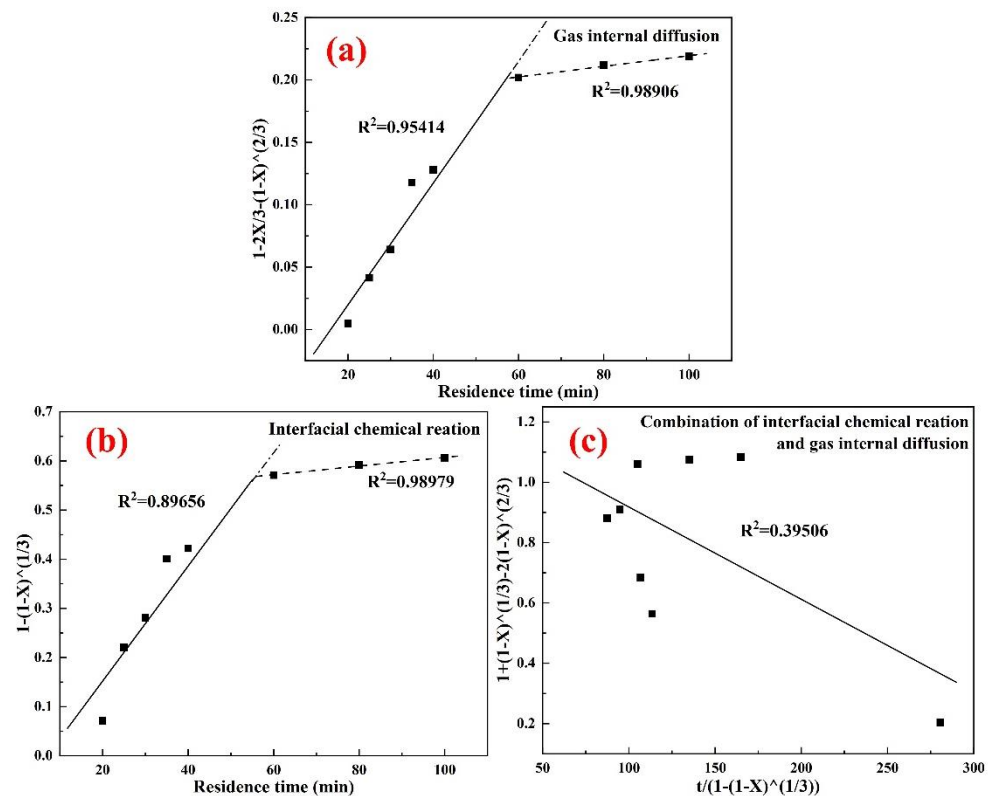


Figure 9. (a) Relationship between $[1 - 2X/3 - (1 - X)^{2/3}]$ and different residence time; (b) Relationship between $[1 - (1 - X)^{1/3}]$ and different residence time; (c) Relationship between $[1 + (1 - X)^{1/3} - 2(1 - X)^{2/3}]$ and $t / [1 - (1 - X)^{1/3}]$.

5. Conclusions

The tin from the tin-bearing iron concentrate could be efficiently removed using a roasting in the mixed atmosphere of CO and SO₂ at 1050 °C. With the partial pressure of SO₂ increased from 0.001 to 0.005, more S₂ was produced from the reduction of SO₂, which in turn promoted the sulfidation and SnO₂ volatilization, resulting in the increased volatilization ratio of Sn from 60.1% to 72.4%. However, the Fe₃O₄ sulfidation also occurred simultaneously at a higher SO₂ partial pressure and an iron sulfide phase was formed, retaining in the roasted iron concentrate, due to which the residual sulfur content increased. The Sn volatilization ratio increased from 27.0% to 80.6% with the increase of roasting temperature from 900 °C to 1050 °C, but it decreased to 74.8% as the roasting temperature was further increased to 1100 °C. It was due to the more formation of a Sn-Fe alloy. The kinetics study showed that the sulfurization of SnO₂ from the concentrated tin-bearing iron was controlled by the internal gas diffusion reaction step. Under the condition of roasting temperature of 1050 °C, SO₂ partial pressure of 0.003, CO partial pressure of 0.003, and residence time of 60 min, the Sn content in the roasted iron concentrate was decreased to 0.032 wt%, and the residual sulfur content was only 0.062 wt%, which meets the BF ironmaking.

Author Contributions: L.L.: Conceptualization, funding acquisition, investigation, methodology, project administration, resources, supervision, writing—original draft, writing—review and editing. Z.X.: Data curation, investigation, validation, writing—original draft. S.W.: Methodology, investigation, validation, writing—original draft. All authors have read and agreed to the published version of the manuscript.

Funding: This study is supported by the National Natural Science Foundation of China (51874153).

Data Availability Statement: All data are available in this study.

Acknowledgments: The authors wish to express their thanks to the National Natural Science Foundation of China (51874153) for their financial support of this research.

Conflicts of Interest: The authors declare no conflict of interest.

References

1. Li, C.; Sun, H.H.; Bai, J.; Li, L.T. Innovative methodology for comprehensive utilization of iron ore tailings: Part 1. The recovery of iron from iron ore tailings using magnetic separation after magnetizing roasting. *J. Hazard. Mater.* **2010**, *174*, 71–77. [[CrossRef](#)] [[PubMed](#)]
2. Wu, F.; Cao, Z.; Wang, S.; Zhong, H. Phase transformation of iron in limonite ore by microwave roasting with addition of alkali lignin and its effects on magnetic separation. *J. Alloys Compd.* **2017**, *722*, 651–661. [[CrossRef](#)]
3. Omran, M.; Fabritius, T.; Elmandy, A.M.; Abdel-Khalek, N.A.; Gornostayev, S. Improvement of phosphorus removal from iron ore using combined microwave pretreatment and ultrasonic treatment. *Sep. Purif. Technol.* **2015**, *156*, 724–737. [[CrossRef](#)]
4. Yu, Y.; Li, L.; Wang, J.Y.; Li, K.Z.; Wang, H. Phase transformation of Sn in tin-bearing iron concentrates by roasting with FeS₂ in CO-CO₂ mixed gases and its effects on Sn separation. *J. Alloys Compd.* **2018**, *750*, 8–16. [[CrossRef](#)]
5. Yu, Y.; Li, L.; Wang, J.Y.; Wang, J.C.; Li, K.Z. Sn separation from Sn-bearing iron concentrates by roasting with waste tire rubber in N₂ + CO + CO₂ mixed gases. *J. Hazard. Mater.* **2019**, *371*, 440–448. [[CrossRef](#)] [[PubMed](#)]
6. Yu, Y.; Li, L.; Sang, X.L. Removing tin from tin-bearing iron concentrates with sulfidation roasting using high sulfur coal. *ISIJ Int.* **2016**, *56*, 57–62. [[CrossRef](#)]
7. Zhang, R.J.; Li, L.; Li, K.Z.; Yu, Y.; Wang, H. Reduction and sulfurization behavior of tin phases in tin-bearing iron concentrates with sulfates in sulfur-bearing stone coal. *ISIJ Int.* **2018**, *58*, 453–459. [[CrossRef](#)]
8. Zhang, R.J.; Li, L.; Li, K.Z.; Yu, Y. Reduction roasting of tin-bearing iron concentrates using pyrite. *ISIJ Int.* **2016**, *56*, 953–959. [[CrossRef](#)]
9. Su, Z.J.; Zhang, Y.B.; Liu, B.B.; Zhou, Y.L.; Jiang, T.; Li, G.H. Reduction behavior of SnO₂ in the tin-bearing iron concentrates under CO-CO₂ atmosphere. Part I: Effect of magnetite. *Powder Technol.* **2016**, *292*, 251–259. [[CrossRef](#)]
10. Wang, Z.W.; Wang, C.Y.; Lu, H.M. Investigation on removal of tin from Sn-bearing iron concentrates by reduction roasting. *Mining Metall.* **2005**, *14*, 63–66. [[CrossRef](#)]
11. Yu, Y.; Li, L. Transformation behaviour of sulfur from gypsum waste (CaSO₄·2H₂O) while roasting with tin-bearing iron concentrate for tin removal and iron recovery. *ISIJ Int.* **2020**, *60*, 2291–2300. [[CrossRef](#)]
12. Pandey, R.; Biswas, R.; Chakrabarti, T.; Devotta, S. Flue gas desulfurization: Physicochemical and biotechnological approaches. *Crit. Rev. Environ. Sci. Technol.* **2005**, *35*, 571–622. [[CrossRef](#)]
13. Bates, T.; Lamb, B.; Guenther, A.; Dignon, J.; Stoiber, R. Sulfur emissions to the atmosphere from natural sources. *J. Atmos. Chem.* **1992**, *14*, 315–337. [[CrossRef](#)]
14. Ma, K.; Deng, J.; Ma, P.; Sun, C.; Zhou, Q.; Xu, J. A novel plant-internal route of recycling sulfur from the flue gas desulfurization (FGD) ash through sintering process: From lab-scale principles to industrial practices. *J. Environ. Chem. Eng.* **2021**, *10*, 106957. [[CrossRef](#)]
15. Lim, J.; Cho, H.; Kim, J. Optimization of wet flue gas desulfurization system using recycled waste oyster shell as high-grade limestone substitutes. *J. Cleaner Prod.* **2021**, *318*, 128492. [[CrossRef](#)]
16. Lim, J.; Choi, Y.; Kim, G.; Kim, J. Modeling of the wet flue gas desulfurization system to utilize low-grade limestone. *Korean J. Chem. Eng.* **2020**, *37*, 2085–2093. [[CrossRef](#)]
17. Li, H.; Zhang, H.; Li, L.; Ren, Q.; Yang, X.; Jiang, Z.; Zhang, Z. Utilization of low-quality desulfurized ash from semi-dry flue gas desulfurization by mixing with hemihydrate gypsum. *Fuel* **2019**, *255*, 115783. [[CrossRef](#)]
18. Fang, D.; Liao, X.; Zhang, X.; Teng, A.; Xue, X. A novel resource utilization of the calcium-based semi-dry flue gas desulfurization ash: As a reductant to remove chromium and vanadium from vanadium industrial wastewater. *J. Hazard. Mater.* **2018**, *342*, 436–445. [[CrossRef](#)]
19. Matsushima, N.; Li, Y.; Nishioka, M.; Sadakata, M.; Qi, H.; Xu, X. Novel dry-desulfurization process using Ca(OH)₂/fly ash sorbent in a circulating fluidized bed. *Environ. Sci. Technol.* **2004**, *38*, 6867–6874. [[CrossRef](#)]
20. Li, Y.; You, C.; Song, C. Adhesive carrier particles for rapidly hydrated sorbent for moderate-temperature dry flue gas desulfurization. *Environ. Sci. Technol.* **2010**, *44*, 4692–4696. [[CrossRef](#)]
21. Zhang, X.; Li, Y.; Zhang, Z.; Nie, M.; Wang, L.; Zhang, H. Adsorption of condensable particulate matter from coal-fired flue gas by activated carbon. *Sci. Total Environ.* **2021**, *778*, 146245. [[CrossRef](#)] [[PubMed](#)]
22. Zhao, Y.; Dou, J.; Duan, X.; Chai, H.; Oliveira, J.; Yu, J. Adverse effects of inherent CaO in coconut shell-derived activated carbon on its performance during flue gas desulfurization. *Environ. Sci. Technol.* **2009**, *54*, 1973–1981. [[CrossRef](#)] [[PubMed](#)]
23. Yao, S.; Cheng, S.; Li, J.; Zhang, H.; Jia, J.; Sun, X. Effect of wet flue gas desulfurization (WFGD) on fine particle (PM_{2.5}) emission from coal-fired boilers. *J. Environ. Sci.* **2019**, *77*, 32–42. [[CrossRef](#)]
24. Zhang, Y.Y. Behaviour Pattern of Stannous Sulfide under Vacuum and High Temperature and Experimental Study of Vacuum Distillation of Sulfur Slag. Master's Thesis, Kunming University of Science and Technology, Kunming, China, 2014.
25. Guo, Y.F. Study on Strengthening of Solid-State Reduction and Comprehensive Utilization of Vanadiferous Titanomagnetite. Ph.D. Thesis, Central South University of Technology, Changsha, China, 2007.

26. Zhang, G.H.; Chou, K.C.; Zhao, H.L. Reduction kinetics of FeTiO₃ powder by hydrogen. *ISIJ Int.* **2012**, *52*, 1986–1989. [[CrossRef](#)]
27. Mo, D.C. *Kinetics for Metallurgy*, 1st ed.; Central South University Press: Changsha, China, 1987; pp. 154–196.
28. Padilla, R.; Sohn, H.Y. The reduction of stannic oxide with carbon. *Metall. Mater. Trans. B* **1979**, *10*, 109–115. [[CrossRef](#)]
29. Zhang, C.F.; Peng, B.; Peng, J. Electric arc furnace dust non-isothermal reduction kinetics. *Trans. Nonferrous Met. Soc. China* **2000**, *10*, 524–530.